Journal of Luminescence 129 (2009) 1568–1574

Contents lists available at ScienceDirect

Journal of Luminescence

journal homepage: www.elsevier.com/locate/jlumin

Optical and EPR study of BaY_2F_8 single crystals doped with Yb

S.M. Kaczmarek [a,*], G. Leniec [a], J. Typek [a], G. Boulon [b], A. Bensalah [b,c]

[a] Institute of Physics, West Pomeranian University of Technology, 17 Al. Piastów, Szczecin, Poland
[b] Physical Chemistry of Luminescent Materials, Claude Bernard/Lyon 1 University, UMR CNRS 5620, Bâtiment A Kastler, 10 rue Amp'ere, 69622 Villeurbanne, France
[c] Institute for Multidisciplinary Research of Advanced Materials, Tohoku University, Sendai 980-8577, Japan

ARTICLE INFO

Available online 8 May 2009

Keywords:
Yttrium barium fluoride
Absorption
Gamma induced absorption
Luminescence
Ytterbium pairs and clusters
Up-conversion

ABSTRACT

Optical and electron paramagnetic resonance study have been carried out on BaY_2F_8 single crystals doped with Yb ions at 0.5 and 10 mol%. The crystals have been obtained using the Czochralski method modified for fluoride crystal growth. Optical transmission measurements in the range of 190–3200 nm and photoluminescence measurements were carried out at room temperature. Absorption spectra of BaY_2F_8 single crystals doped with Yb due to the $^2F_{7/2} \rightarrow {}^2F_{5/2}$ transitions have been observed in the 930–980 nm range. To analyze the possible presence of Yb^{2+} ions in the investigated crystals, irradiation with γ-quanta with a dose of 10^5 Gy have been performed. The observed photoluminescence bands show usual emission in IR and other one in VIS, being an effect of cooperative emission of Yb^{3+} ions and energy up-conversion transitions of photons from IR to UV–vis(visible) due to hoping process between energy levels of paired Yb^{3+} and Er^{3+}, where Er^{3+} ions are unintentional dopants. The EPR spectra of BaY_2F_8:Yb 10 mol% consist of many overlapping lines. They have been analyzed in terms of spin monomers, pairs, and clusters. The angular dependence of the resonance lines positions have been studied also to find the location of coupled ytterbium ions in the crystal structure.

1. Introduction

The BaY_2F_8 (BYF) single crystal doped with trivalent rare-earth ions has recently attracted a lot of attention because of its potential application as VUV scintillators, as media for solid-state lasers in VUV and IR, as new efficient phosphors for plasma display panels and luminescent lamps based on rare-gas discharges [1,2]. Two of the most important features of this crystal are the very low phonon energy ($\sim$350 cm^{-1}) that makes it suitable for laser application in the near IR region, and low thermal lensing. Due to a very simple energy scheme of ytterbium ion, it is possible to avoid up-conversion or excited state absorption and concentration quenching within a large domain. Recent interesting results obtained thanks to the high-purity of BYF crystals allowed to use it as an effective optically cooling material. In all cases, the host matrix is exposed to high fluxes of pumping radiation in the UV/(vis) visible spectral regions or to high-energy photons or particles. Such conditions can easily result in optical damage of the material, giving rise to degradation of its application-related characteristics and performance. The study of color center creation using optical spectroscopy is then a useful approach, which can be applied to understand the relevance of such degradation processes and their microscopic mechanisms. In the case of high-power laser applications, the host materials are exposed to laser diode pumping and must withstand that high-intensity irradiation without changing their transmission characteristics.

The symmetry of the BYF crystal is monoclinic (space group C^3_{2h}–C2/m with the following lattice parameters: $a = 0.6972$ nm, $b = 1.0505$ nm, $c = 0.4260$ nm, and $\beta = 99°45'$ [3]). The unit cell contains two units [4]. The Y^{3+} ion lattice site (in International Tables for Crystallography, the site has Wyckoff letter *g*, multiplicity 4, and site symmetry 2) is surrounded by eight F^- anions forming slightly deformed Thompson cube. Yttrium polyhedra, sharing a common edge, form parallel (0 0 1) planes consisting of six-segmented rings (Fig. 1). Substituting ion may occupy mainly Y^{3+} sites that are all crystallographically equivalent, but some discrepancies from C_2 local point symmetry of the ytterbium ion in BYF matrix due to e.g. high concentration and lattice defects could be expected.

High doping of the crystals for laser purposes results in creation of some new defect centers, such as pairs of doped ions and their clusters. The electron paramagnetic resonance (EPR) method is very sensitive to the presence of such kind of centers, if they are paramagnetic in nature. The aim of the paper is analysis of the defect structure of the BYF single crystal doped with ytterbium, using optical spectroscopy and EPR methods. As the doping level of Yb^{3+} ions in BYF is rather high, a special attention will be paid to find spectroscopic evidences of the presence of paramagnetic pairs in this material.

* Corresponding author.
E-mail address: skaczmarek@ps.pl (S.M. Kaczmarek).

0022-2313/$ - see front matter © 2009 Elsevier B.V. All rights reserved.
doi:10.1016/j.jlumin.2009.04.063

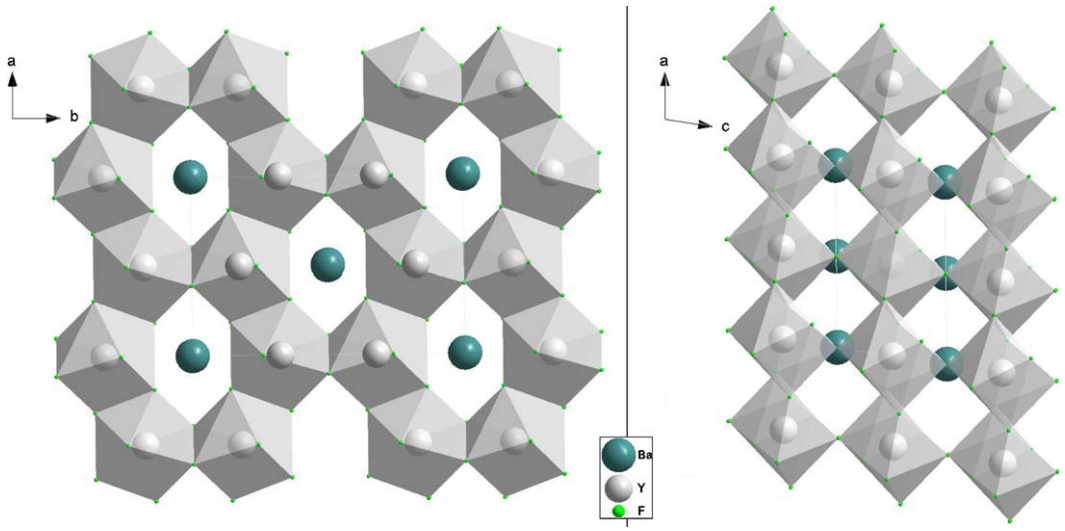

Fig. 1. Projection of the BaY_2F_8 structure on the *ab* plane (right) and *ac* plane (left).

2. Experimental

The BaY_2F_8 single crystals were obtained using the Czochralski method modified for fluoride crystal growth in Tohoku University, Japan [5]. Samples used for the spectroscopic measurements were cut from the crystals as parallel plates with surfaces perpendicular to the *c*-axis, both polished, 1 mm in thickness. To analyze the presence of Yb^{2+} ions in the investigated crystals, irradiation of the crystals with γ-quanta with a dose of 10^5 Gy have been performed. Under influence of γ-radiation Yb^{3+} ions may capture Compton electrons, forming Yb^{2+} ions. So, the samples were examined for the absorption prior to and after γ-irradiation with a dose of 10^5 Gy. Additional absorption was calculated according to the formula

$$K(\lambda) = \frac{1}{d} \ln\left(\frac{T_1}{T_2}\right) \quad (1)$$

where T_1 and T_2 are transmissions of a sample measured prior to and after γ-irradiation, respectively, *d*—sample thickness, *K*—absorption, and λ—wavelength. Transmission measurements were performed at room temperature using Lambda-900 of Perkin-Elmer spectrophotometer in the range of 190–3200 nm. The photoluminescence (PL) measurements were carried out using a SS-900 Edinburgh Inc. spectrophotometer, both in the Institute of Optoelectronics, Military University of Technology, Warsaw, Poland.

The EPR spectra were recorded on a conventional X-band Bruker ELEXSYS E 500 CW-spectrometer operating at 9.5 GHz with 100 kHz magnetic field modulation. Rectangular sample cut out from bulk crystal for the EPR purposes had dimensions $2.4 \times 2.4 \times 2.9\ mm^3$, where the largest dimension was chosen along the axis perpendicular to the *ab*-plane. The sample was glued to a quartz pipe, placed into the resonator chamber and rotated around perpendicular axes. The laboratory axes system (*xyz*) was chosen in the following way: the *x*-axis was oriented along the crystallographic *a*-axis, the *y*-axis along the crystallographic *b*-axis, and the *z*-axis was perpendicular to the *xy* plane. The first derivative of the absorption spectra have been recorded as a function of the applied magnetic field. Temperature dependence of the EPR spectra in the 3–300 K temperature range was recorded using an Oxford Instruments ESP helium-flow cryostat.

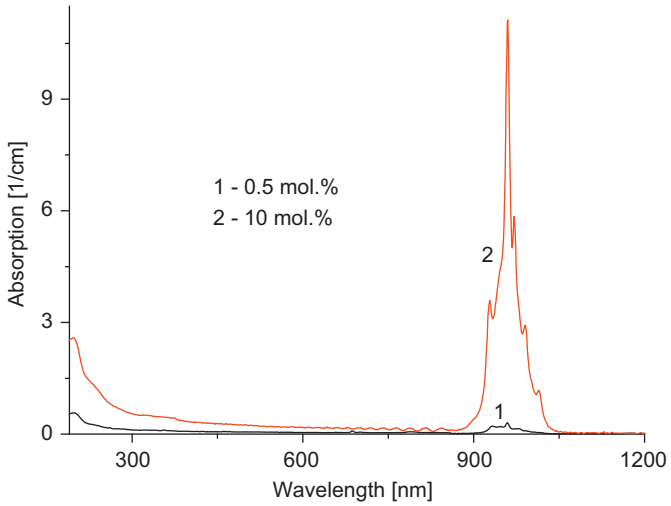

Fig. 2. The absorption bands of BaY_2F_8:Yb: 1–0.5 mol% Yb and 2–10 mol% Yb.

3. Results and discussion

3.1. Optical investigations

The interpretation of the Yb^{3+} energy levels in the different fluoride hosts turned out to be difficult mainly because of a strong phonon–electron coupling of Yb^{3+} ion which results in the appearance of additional peaks making the interpretation of the different absorption and emission lines complex, especially at room temperature. Room temperature absorption spectra of Yb^{3+} in BYF single crystals due to the $^2F_{7/2} \rightarrow {}^2F_{5/2}$ transition are presented in Fig. 2. The intense, well-resolved bands are observed at 930, 948, 960 (high intensity), and about 980 nm. Some weak bands could be also recognized due to vibronic transitions as observed in various Yb^{3+}-doped oxides [6–8]. Taking into account low temperature results of the absorption spectrum, the Yb^{3+} energy levels are as follows: $^2F_{7/2}$ (0, 216, 430, and 530 cm^{-1}), $^2F_{5/2}$ (10,277, 10,395, and 10,735 cm^{-1}) [5]. The intensity of the bands strongly depends on the Yb^{3+} intentional concentration. No clearly observed Yb^{2+} or Er^{3+} absorption bands are present.

BYF:Yb belongs to the class of wide band gap materials. Fundamental absorption edge lay below 190 nm, while the band energy gap equals $E_g = 5.75$ eV for 0.5 mol% Yb and $E_g = 5.58$ eV for 10 mol% Yb.

The results of the investigations of γ-induced absorption of low and highly doped BYF:Yb (1–0.5 and 2–10 mol%, respectively) crystals are presented in Fig. 3. The registered additional absorption bands are characteristic for Yb^{2+} ions (e.g. 340 nm) and color centers (e.g. 440 nm). It could be concluded that in the Yb^{3+}-doped BYF, Yb^{2+} are created by γ-irradiation, giving rise to the absorption bands in 200–380 nm range. As one can see from Fig. 3, the higher is the ytterbium concentration the lower is an additional absorption. It confirms previous results obtained for $LiLuF_4$ and $LiYF_4$ fluoride single crystals doped with ytterbium that color centers compete with Yb^{3+} ions in capturing of Compton electrons [9]. Moreover, in the range of IR absorption, one can observe some changes in the absorption characteristic to a valence change ($Yb^{3+} \rightarrow Yb^{2+}$) of ytterbium ions within Yb^{3+}–Yb^{3+} pair (see 900–1100 nm wavelength region) [10].

Thus, after γ-irradiation with a dose of 10^5 Gy, we observe induced absorption bands very similar to that recorded in the CaF_2:Yb crystal [10]. Yb^{2+} centers that respond for the induced absorption spectra of BYF crystals low and highly doped with Yb, favors Yb^{2+} ions related to Yb^{3+}. It is possible that Compton electrons formed by γ-quanta are more easily captured by Yb^{3+} pairs present in BYF crystals doped with Yb^{3+} ions than by isolated Yb^{3+} ions.

PL of highly doped with ytterbium BYF: (10 mol% Yb^{3+}) "as-grown" (1) and γ-irradiated (2) crystal is presented in Fig. 4a. The figure shows emission of the crystal in the UV being excited in the IR. Room temperature emission spectra in the IR do not differ from the spectra of 2.5 mol% BYF:Yb single crystal presented elsewhere [4]. As one can see in Fig. 4a, some well-resolved bands are observed between 200 and 800 nm. Most of these bends are very similar to the bands of Yb^{3+} and Er^{3+} ions interacting by energy up-conversion transitions (EUT) excluding emission band centered at about 480 nm [11]. The observed emission is Er^{3+} ions emission as an effect of EUT process (see Fig. 4b) and in a case of 480 nm band it is cooperative emission of Yb^{3+} ions. It is observed that γ-radiation (curve 2) leads to an increase in the amount of Er^{3+} luminescence centers (the curves are normalized each other). However, not all of the energy levels are equally excited. It may indicate on the presence of both: isolated Er^{3+} ions and others, forming pairs with Yb^{3+}.

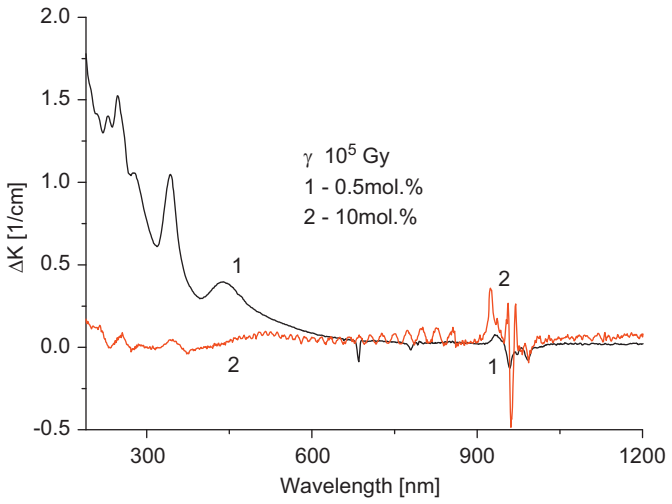

Fig. 3. γ-induced absorption bands of BaY_2F_8:Yb: 1–0.5 mol% and 2–10 mol%.

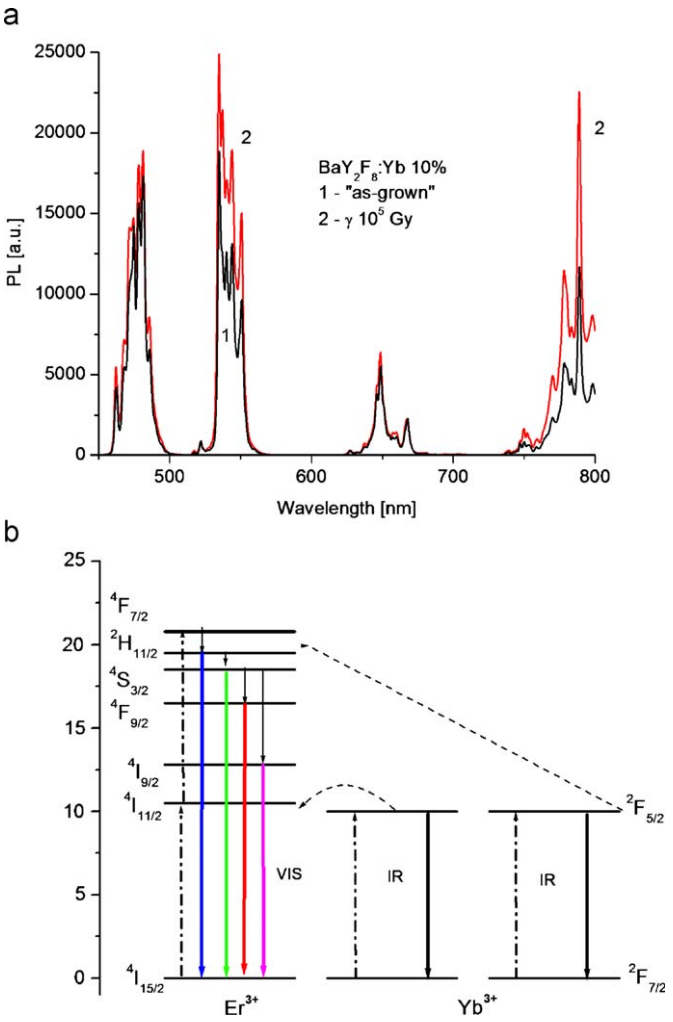

Fig. 4. (a) PL spectrum of BaY_2F_8:Yb (10 mol%): 1—"as-grown" crystal, 2—γ-irradiated with a dose of 10^5 Gy. $\lambda_{ex} = 980$ nm. (b) Schematic diagram of Yb^{3+}-sensitized Er^{3+} up-conversion luminescence above 500 nm wavelength.

For low-doped BYF:Yb (0.5 mol%) crystals, we have not observed similar PL in case of as-grown crystal while a weak one only for γ-irradiated.

3.2. EPR measurements

Free Yb^{3+} ion has a $4f^{13}$ electronic configuration. The free-ion Hamiltonian (incorporating electron–electron and spin–orbit interaction terms) produces the $^{2S+1}L_J$ multiplets separated by about 10^3–10^4 cm^{-1}. According to the Hund's rules, the ground state is $^2F_{7/2}$ and the excited state is $^2F_{5/2}$. The crystal field of the host material removes the $2J+1$ degeneracy of the $^{2S+1}L_J$ states and gives twofold degenerate states called the Kramers doublets, separated by about 10–10^2 cm^{-1}. This degeneracy could be lifted by an external magnetic field B. At liquid helium temperature, only the lowest doublet is populated, and thus the EPR spectrum can be described by a Hamiltonian with an effective spin $S = \frac{1}{2}$. In addition to even isotopes (nuclear spin $I = 0$, natural abundance 69%), ytterbium has two odd isotopes which give rise to hyperfine structure, ^{171}Yb with nuclear spin $I = \frac{1}{2}$ (natural abundance 14.4%) and ^{173}Yb with nuclear spin $I = \frac{5}{2}$ (natural abundance 16.6%). The resulting effective spin Hamiltonian of the Yb^{3+} monomers is

$$H_{mon} = \beta BgS + SAI \quad (2)$$

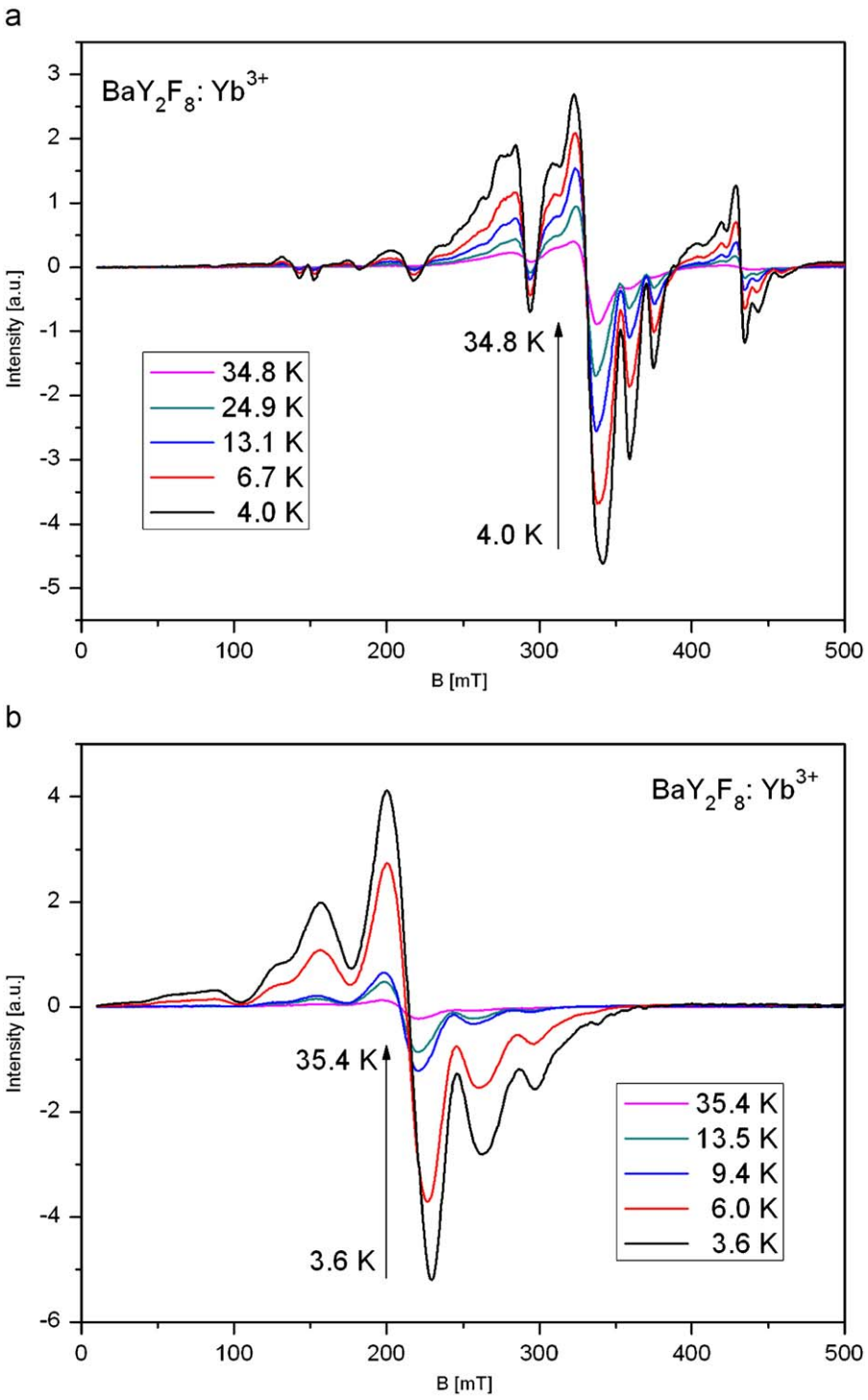

Fig. 5. EPR spectra of BaY_2F_8:Yb crystal for several temperatures and an external magnetic field directed along the *x*-axis (crystallographic *a*-axis, *yz* plane) (a), and in the *xz* plane (b).

where β is the Bohr magneton and g and A are tensors. The first term in Eq. (2) is called the Zeeman term and the second the hyperfine interaction term.

As the doping level of Yb in BYF is high, the existence of Yb pairs and clusters should be considered. For pairs of similar ions (two coupled Yb^{3+} ions in neighboring sites A and B), the following Hamiltonian is relevant [12]

$$H_{pair} = \beta B g^A S^A + \beta B g^B S^B - 2J S^A S^B + S^A D_{dd}^{AB} S^B \quad (3)$$

where the two first terms are the Zeeman terms, the third is an isotropic part (Heisenberg type) of the exchange interaction and the fourth term is the magnetic dipole–dipole interaction. In Eq. (3), J is the isotropic exchange interaction constant that is usually not directly calculated from the EPR spectrum. When J is of the order of kT, it could be determined from the temperature dependence of the EPR signal intensity. Otherwise, it could be measured by high-resolution spectroscopy (when J is large enough) or from EPR hyperfine spectrum in case of paramagnetic

species with nuclear magnetic moments. The dipolar tensor has the following well-known expression [12]:

$$D_{dd}^{AB} = \frac{\mu^A \mu^B}{R^3} - \frac{3(\mu^A R)(\mu^B R)}{R} \quad (4)$$

where the magnetic dipole moments are written as $\mu^{A,B} = \beta g^{A,B} S^{A,B}$. Eq. (4) allows calculation of the distance R between neighboring two ions forming a pair. In particular, for magnetic field B parallel to the pair's axis two transitions at magnetic fields $B_{\pm}$ are expected from the dipole–dipole Hamiltonian [13]

$$B_{\pm} = B_0 \left[1 \pm \frac{(-2D_1 + D_2)}{g_{\parallel} \beta B_0} \right] \quad (5)$$

where the dipolar parameters D_1 and D_2 are given by the following equations:

$$D_1 = \frac{\beta^2(-g_{\parallel}^2)}{2R^3} \quad D_2 = \frac{\beta^2(g_{\perp}^2)}{2R^3} \quad (6)$$

In Eq. (5), B_0 is the center magnetic field of the dipolar doublet. Fig. 5 presents a few of the EPR spectra registered at different temperatures, for two specific orientations of the external magnetic field relative to the crystallographic axes.

The observed EPR spectrum consists of many overlapping lines, mainly in the 250–450 mT range. It resembles in many ways the spectrum of rare-earth pairs registered e.g. for $CsCdBr_3$:Yb [13]. With increasing temperature, the intensity of the lines quickly decreases and above 50 K the EPR spectrum is hardly visible. This is to be expected for the rare-earth ions due to a strong increase with temperature of the relaxation rates of the spin system. There is also a large variation of the resonance lines positions due to changes of the external field orientation relative to crystallographic axes (Figs. 5a and b).

In Fig. 6, the angle dependence of selected, relatively well-separated EPR lines observed in the *xy* plane (*ab* crystallographic plane) is presented. This angular dependence shows that the resonance lines have axial symmetry about the crystallographic *b*-axis. The angle dependence also enables to group the resonance lines into two sets: one set contains the lines that are attributed to separated Yb^{3+} ions and the other to the Yb^{3+} pairs. The lines attributed to pairs should have $(3\cos^2\varphi - 1)$-type dependence, where φ is the angle between magnetic field and the pair axis. The

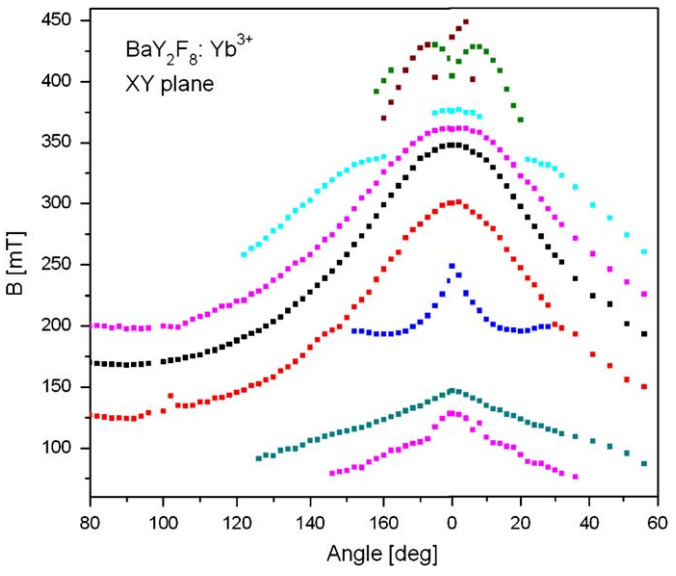

Fig. 6. Angle dependence of the EPR lines observed in BaY_2F_8:Yb crystal in the *xy* plane (*ab* crystallographic plane).

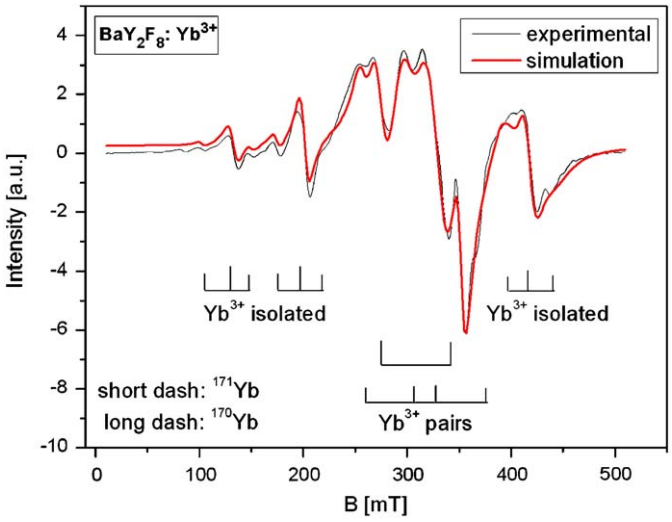

Fig. 7. Comparison of experimental and simulated spectra of BaY_2F_8:Yb crystal registered at 23 K for external magnetic field directed along the *z*-axis.

Table 1
Values of spin Hamiltonian parameters of the observed paramagnetic centers in BaY_2F_8:10% Yb single crystal.

	Parameter	Value		
Yb^{3+} monomers	$g_{\parallel}$	4.91	3.34	1.73
	$g_{\perp}$	5.09	3.34	1.61
Yb^{3+}–Yb^{3+} pair	$g_{\parallel}$	2.216		
	$g_{\perp}$	2.241		
	D_1 (10^{-4} cm^{-1})	235.14		
	D_2 (10^{-4} cm^{-1})	229.92		
	R [Å]	3.59		

ytterbium monomers might show a different type of pattern in the angle dependence.

Fig. 7 shows the results of the fitting of the observed spectrum registered at 23 K for magnetic field directed along the *z*-axis. Although there are differences between experimental (narrow line) and simulated spectra (thick line), the main features of the EPR spectrum are reproduced correctly.

The most intense lines observed in 250–400 mT range of magnetic field were attributed to Yb^{3+} pairs, while the low and high-field lines to the three different monomeric Yb^{3+} paramagnetic centers. In the simulation, the Lorentzian-shaped lines with different intrinsic linewidths were applied. The values of the relevant spectral parameters for the observed monomeric and dimeric centers are presented in Table 1. From the calculated D_1 and D_2 dipole parameters, the distance between ions forming a pair could be calculated by using Eq. (6). The obtained value, $R = 3.58$ Å, seems to be reasonable if compared to the Y interionic separation distance in the BYF crystal.

In Fig. 8 the location of the Yb^{3+} pair is proposed. The two Yb^{3+} ions forming a pair are assumed to enter substitutionally at Y sites. In that case there is no problem with charge compensation and the ionic radii of both ions in eightfold coordination are similar ($r(Y^{3+}) = 1.015$ Å, $r(Yb^{3+}) = 0.98$ Å [14]). The distances between six neighboring Y^{3+} ions forming the ring in *ab*-plane (designated as Y_1–Y_6 in Fig. 8) are not the same: the distances Y_1–Y_2 and Y_4–Y_5 are equal ($L_1 = 3.68$ Å) and different from Y_2–Y_3, Y_3–Y_4, Y_5–Y_6, and Y_6–Y_1 distances ($L_2 = 3.80$ Å). It is proposed that the Yb^{3+} pair generating the observed EPR spectrum is placed at

Y_1–Y_2 and Y_4–Y_5 sites There are two main arguments for selecting such location: the axis of a pair should be directed along the *b* crystallographic axis (it follows from the rotational diagram) and the calculated separation between Yb^{3+} ions in a pair (3.59 Å) is closer to that particular interionic yttrium distance. The smaller separation in the Yb^{3+} pair could be mostly accounted for by a smaller ionic ion radius of the substituting ion so the relaxation effect should play only a minor role.

It is more difficult to propose the locations of paramagnetic centers attributed to the monomeric Yb^{3+} species, because there are many possibilities in the crystallographic structure of BYF to accommodate these centers. They could be associated with a single Yb^{3+} ions substituting for Y^{3+} ion at any of the Y_1–Y_6 sites or forming the Yb^{3+}–Yb^{2+} pair located at two neighboring Y sites. Due to the mentioned above differences in Y–Y distances, the substitution of that pair in e.g. Y_1–Y_2 or Y_1–Y_6 positions would produce two magnetically inequivalent paramagnetic centers.

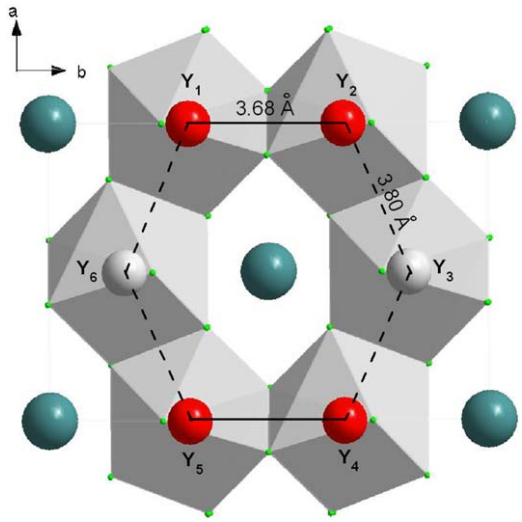

Fig. 8. Schematic representation of Yb pairs location in BaY_2F_8:Yb structure.

Analysis of the temperature dependence of the integral intensity *I* of the EPR spectra has also been carried out. The integral intensity is calculated as an area under the absorption EPR spectrum (not the usual first derivative) and is proportional to the spin susceptibility of the paramagnetic species taking part in resonance. For the magnetic field having the same orientation relative to the crystalline axes as represented in Fig. 5b, one can exclude the presence of Yb pairs in EPR spectra. For the EPR spectra registered in that orientation, the fitting of $I(T)$ to the Curie–Weiss law

$$I(T) = \frac{C'}{T - T_c} \tag{7}$$

where C' is a constant and T_c is the Curie–Weiss temperature. The fitting gave quite satisfactory results for $T_c = 1.11$ K (see Fig. 9). This type of $I(T)$ is expected for interacting spin monomers (T_c describes the strength of magnetic interaction and the positive sign of it indicates on the presence of ferromagnetic interaction), but also for spin clusters.

In that crystal orientation, for which EPR spectra are presented in Fig. 5a (pair presence), we have obtained good enough fitting assuming a joint presence of Yb pairs ($x = 0.8$) and clusters ($1-x = 0.2$) (Fig. 10). These values were calculated from fitting to the following function containing two terms:

$$I(T) = xI_1(T) + (1 - x)I_2(T) \tag{8}$$

where

$$I_1(T) = \frac{C_1}{T}\left[1 + \frac{1}{3}\exp\left(-\frac{2J_d}{T}\right)\right]^{-1} \tag{9}$$

$$I_2(T) = \frac{C_2}{T}\exp\left(-\frac{T_0}{T}\right) \tag{10}$$

Eq. (9) is a well-known Bleaney–Bowers expression for integral EPR intensity, applied often in the case of paramagnetic species forming dimers [15], while Eq. (10) is used to fit of $I(T)$ when

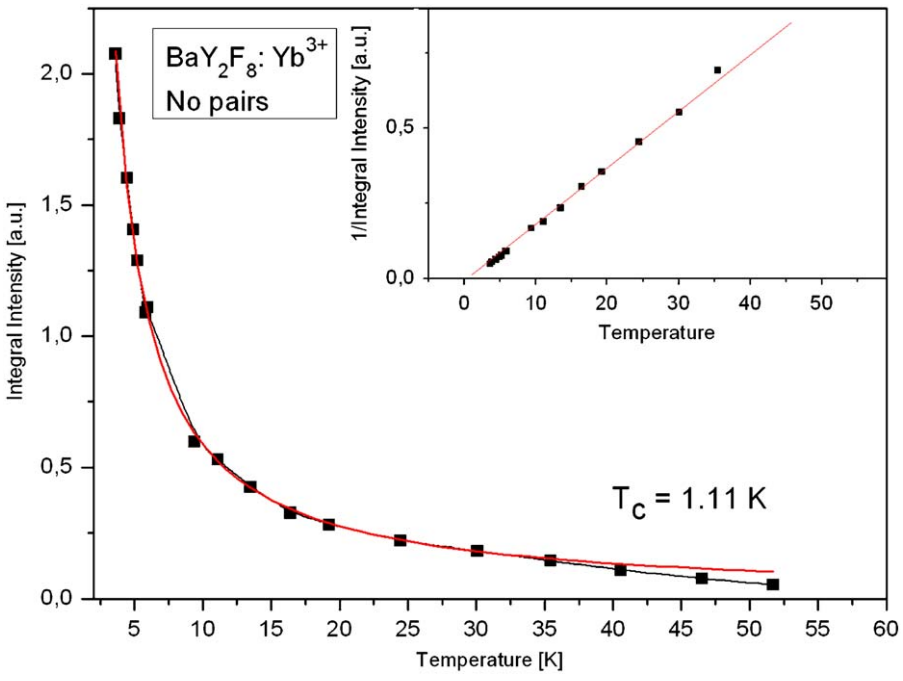

Fig. 9. Temperature dependence of the integral intensity of the EPR spectra presented in Fig. 5b and the fitting with the Curie–Weiss law. In insert, the reciprocal of integrated intensity is presented.

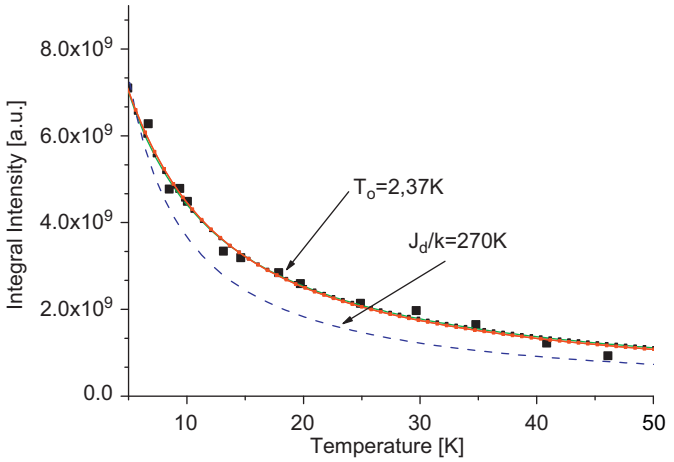

Fig. 10. Temperature dependence of the integral intensity of the EPR spectrum presented in Fig. 5a (filled squares are experimental points). The dashed line represents the fit to the experimental points assuming the presence of pairs (Eq. (9), with $J_d/k = 270$ K), while the solid line is the fit only with clusters (Eq. (10), with $T_0 = 2.37$ K). The dotted curve represents the fit with Eq. (8), with $x = 0.8$, $T_0 = 2.37$ K, and $J_d/k = 270$ K.

paramagnetic ions form clusters with a nonmagnetic ground state [16]. In the above functions, J_d is the antiferromagnetic interdimer coupling and T_o is the difference of energy (expressed in K) between the ground state and the excited state. The best fit was achieved for $J_d/k = 270(5)$ K and $T_o = 2.37(2)$ K. It follows that the dominating contribution to the EPR spectra comes from the ytterbium dimers, but the assumption of the presence of clusters significantly improves the fit (see Fig. 10). The above conclusion agrees very well with results of optical measurements. In the PL spectrum, we have observed bands that could be assigned to Yb dimers and/or clusters. The PL band which is observed in the spectrum with a maximum at about 480 nm may be the effect of the presence of ytterbium pairs in the investigated crystals.

4. Conclusions

Room temperature absorption and PL spectra of Yb^{3+}-doped BaY_2F_8 crystals due to the $^2F_{7/2} \rightarrow {}^2F_{5/2}$ transitions have been recorded. Besides usual emission in IR, vis emission being an effect of cooperative emission of Yb^{3+}–Yb^{3+} pairs and EUT from Yb^{3+} to uncontrolled Er^{3+} ions was observed.

Yb^{2+} ions are created in the crystals by γ-irradiation within Yb^{3+} pairs of ions, giving rise to absorption bands in the 200–380 nm range.

EPR measurements of the BYF single crystals doped with Yb have revealed a rich spectrum of magnetic and nonmagnetic ytterbium centers. Analysis of the EPR spectra taken with the external field in different directions relative to the BYF structure permitted to identify at least three different Yb^{3+} monomers. It confirmed the presence of the Yb^{3+}–Yb^{3+} pairs and clusters, and indicated on their possible location in the crystal lattice. Temperature dependence of integral EPR intensity enabled calculation of parameters that indicate on an important role of spin dimers and clusters.

Acknowledgement

Authors deeply acknowledge to Prof. Jorma Holsa for fruitful discussion.

References

[1] S. Wiitwer, M. Pollnau, R. Spring, W. Luthy, H.P. Weber, R.A. McFarlane, Ch. Harder, H.P. Meier, Opt. Commun. 132 (1996) 107.
[2] N.Yu. Kirikova, V.E. Klimenko, V.A. Kozlov, V.N. Makhov, N.M. Khaidukov, T.V. Uvarova, Nucl. Instrum. Methods. Phys. Res. A 359 (1995) 351.
[3] N.L. Tkachenko, L.S. Garashinova, O.E. Izotova, V.B. Aleksandrov, B.P. Sobolev, J. Solid State Chem. 8 (1973) 213.
[4] S. Bigotta, T. Parisi, L. Bonelli, A. Toncelli, A. Di Lieto, M. Tonelli, Opt. Mater. 28 (2006) 1321.
[5] A. Bensalah, M. Ito, Y. Guyot, C. Goutadier, A. Jouini, A. Brenier, H. Sato, T. Fukuda, G. Boulon, J. Lumin. 122–123 (2007) 444.
[6] A. Lorenzo, H. Joffresic, B. Roux, G. Boulon, J. Garcia-Sole, Appl. Phys. Lett. 67 (1995) 3735.
[7] P.H. Haumesser, R. Gaume, B. Viana, E. Antic-Fidancev, D. Vivien, J. Phys.: Condens. Matter 13 (2001) 5427.
[8] R. Gaume, P.H. Haumesser, B. Viana, D. Vivien, B. Ferrand, G. Aka, Opt. Mater. 19 (2002) 81.
[9] S.M. Kaczmarek, A. Bensalah, G. Boulon, Opt. Mater. 28 (1–2) (2006) 123.
[10] S.M. Kaczmarek, T. Tsuboi, M. Ito, G. Boulon, G. Leniec, J. Phys.: Condens. Matter 17 (2005) 3771.
[11] Iko Hyppanen, Jorma Hölsa, Jouko Kankare, Mika Lastusaari, Laura Pihlgren, Ann. N.Y. Acad. Sci. 1130 (2008) 267.
[12] O. Guillot-Noel, Ph. Goldner, P. Higel, D. Gourier, J. Phys.: Condens. Matter 16 (2004) R1.
[13] V. Mehta, O. Guillot-Noel, D. Simons, D. Gourier, Ph. Goldner, F. Pelle, J. Alloys Compd. 323 (4) (2001) 308.
[14] R.D. Shannon, Acta Crystallogr. A 32 (1976) 751.
[15] B. Bleaney, K.D. Bowers, Proc. R. Soc. London A 214 (1952) 451.
[16] J. Yoshikawa, C. Urakawa, H. Ohta, T. Koide, T. Kawamoto, Y. Fujiwara, Y. Takeda, Physica E 10 (2001) 395.